

# Some consequences of high temperature water vapor spectroscopy: Water dimer at equilibrium

M. Yu. Tretyakov<sup>a)</sup> and D. S. Makarov<sup>b)</sup>

*Institute of Applied Physics of the Russian Academy of Sciences, 46 Ulyanov str.,  
Nizhny Novgorod 603950, Russia*

(Received 3 November 2010; accepted 31 January 2011; published online 23 February 2011)

It is shown that the evolution of water vapor spectra in the 2500–5000  $\text{cm}^{-1}$  range recorded at 650 K and pressures up to 130 atms after subtraction of monomer contribution may be interpreted qualitatively well on the basis of experimental data on water dimer and trimer obtained from cold molecular beams and in He droplets. The proposed spectroscopic model considers water vapor as a mixture of nonideal monomers, dimers, and trimers at chemical equilibrium. The effect of line mixing is taken into account in the monomer spectrum modeling. Decomposition of the high temperature spectra allowed determining a dimer equilibrium constant that was compared with the previously known values. The contribution of water trimer is assessed. The performed analysis indicates that the number of bound dimers in water vapor is quite large, even at such a high temperature. © 2011 American Institute of Physics. [doi:10.1063/1.3556606]

## I. INTRODUCTION

The role of water dimer in atmospheric absorption has been widely discussed since the 1960s when Viktorova and Zhevakin put forward a conjecture that the dimer is a cause of extra absorption in atmospheric windows of transparency at millimeter waves.<sup>1</sup>

The dimer spectrum was first observed in microwave range in cold molecular beams by Dyke and Muentert.<sup>2</sup> This method of dimer study was successfully used by many other research groups (see Ref. 3 and references therein). A large number of resolved spectral lines were observed and interpreted. However, these observations of the dimer in nonequilibrium conditions do not give information about width and shape of rotational–vibrational bands of the dimer and about its abundance in ambient conditions.

Attempts of experimental observation of dimer spectrum (or at least an evidence of dimer presence) at close to atmospheric equilibrium conditions have been the subject of a great number of publications since the appearance of the dimeric hypothesis (Ref. 1). The conclusions resulting from the undertaken studies were less reliable than those from observation in molecular beams and often contradicted each other. Some of them were later revoked (e.g., Refs. 4–6). Discussion of possible contribution of the dimer to the water continuum in the IR range and related references can be found, for example, in the recent review papers.<sup>7</sup> Estimation of the dimer contribution to near-infrared and visible solar radiation absorption in atmosphere can be found, e.g., in Ref. 8. However, the role of the dimer in atmospheric absorption and as a consequence in the radiation balance of the Earth still remains uncertain.

The spectroscopy of supercritical water is an alternative direction of experimental studies of the water dimer at equilibrium. Its experimental conditions ensure a considerable fraction of the dimer in the studied sample. Such studies in the IR range were undertaken by several groups (e.g., Refs. 9–12). Their results are in reasonable agreement with each other. However, interpretation of these spectra is hampered, on the one hand, by close coincidence of vibrational frequencies of the monomer and the dimer (as well as higher-order water associates) and as a consequence by strong overlapping of rovibrational bands of these molecules and, on the other hand, by difficulties of accounting for collisional broadening and coupling of monomer lines under these extreme conditions. As a result, only some very general conclusions about the dimer properties were made from analysis of these spectra.

Also worth mentioning is a considerable recent progress of *ab initio* calculations of the dimer by several research groups. The equilibrium constant,<sup>13</sup> inter- and intramolecular vibrational modes (see, e.g., Refs. 14 and 15), and even the entire millimeter wave and far infrared spectrum of the dimer were calculated. The most accurate calculation of the spectrum was reported by Scribano and Leforestier.<sup>16</sup> The calculation covers range of wave numbers from 0 up to 600  $\text{cm}^{-1}$ . Analysis of the latter spectrum leads to the conclusion<sup>17</sup> that the rotational structure of the dimer spectrum resolved under equilibrium conditions close to the atmospheric ones can be potentially observed by resonator spectrometer.<sup>18</sup> However, because of limited sensitivity, the possibility of the observation directly depends on the value of the dimer equilibrium constant. A most complete comparative analysis of available theoretical and experimental data on the value of the constant at different temperatures is given in Ref. 13. The analysis demonstrates that this value is rather uncertain.

The subject of the present paper is an attempt of accurate spectroscopic reanalysis of supercritical water spectra in

<sup>a)</sup> Author to whom correspondence should be addressed. Electronic mail: trt@appl.sci-nnov.ru. URL: <http://www.mwl.sci-nnov.ru>.

<sup>b)</sup> Electronic mail: dmak@appl.sci-nnov.ru. URL: <http://www.mwl.sci-nnov.ru>.

the O-H fundamental stretching region using positions and intensities of the dimer rovibrational bands, which were recently found experimentally at low temperatures in helium droplets.<sup>19</sup> Experimental spectra in the 2500–5000 cm<sup>-1</sup> range recorded by Jin and co-workers<sup>12,20</sup> at 650 K and pressures up to 130 atms were used for the analysis. The final practical goal of the analysis is verification of the dimer equilibrium constant.

## II. THEORETICAL MODEL

Theoretical analysis of the observed spectrum assumes knowledge of shape and integrated intensity of its constituents. Total integrated intensity ( $I$ ) and absorption coefficient ( $\alpha$ ) can be represented in the following general form:

$$I = \int \alpha(\nu) d\nu = I_m + I_d + I_t + \dots$$

$$= n_m \sigma_m + n_d \sigma_d + n_t \sigma_t + \dots, \quad (1)$$

$$\alpha(\nu) = \alpha_m(\nu) + \alpha_d(\nu) + \alpha_t(\nu) + \dots$$

$$= n_m \sigma_m \Phi_m(\nu) + n_d \sigma_d \Phi_d(\nu) + n_t \sigma_t \Phi_t(\nu) + \dots, \quad (2)$$

$$n = n_m + n_d + n_t + \dots, \quad (3)$$

where indices  $m$ ,  $d$ , and  $t$  correspond to monomer, dimer, and trimer;  $\sigma$  is absorption cross section,  $n$  is molecular density; and  $\Phi(\nu)$  is the normalized shape of the absorption band:

$$\int_{\text{band}} \Phi(\nu) d\nu = 1.$$

Detailed elaboration of the model requires consideration of some of its building blocks.

### A. Equation of state of water vapor

Figure 1 presents water vapor pressure *versus* density at the experimental temperature as follows from the virial equations of state truncated after the term with the first, second, and third virial coefficients. Comparison of the first two curves shows that the amount of water dimers under the conditions of the experiment is expected to be really significant. Discrepancy between the curves constitutes 1% at about 7 atms and is more than 30% at upper experimental pressures. The second and third curves start to diverge noticeably at about 50–60 atms and at 130 atms the difference reaches about 3%. This indicates that even at such relatively low pressures of water vapor we may expect not only manifestations of water dimer but also higher-order water associates. The semiempirical International Association for the Properties of Water and Steam (IAPWS) formulation of water vapor state<sup>21</sup> is also shown in Fig. 1 as an accurate reference.

The treatment of water vapor as a mixture of small water clusters (monomer, dimer, trimer, etc.) requires answering the question whether monomolecular gas of each constituent of the mixture is real or ideal. We suppose that molecular

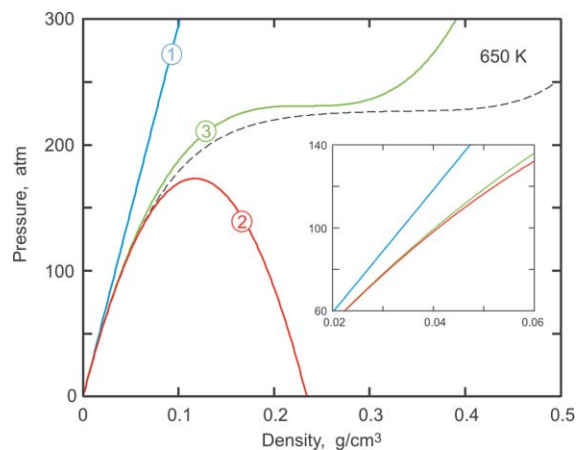


FIG. 1. Virial equation of state curves for water vapor at 650 K. Curves 1, 2, 3 correspond to the equation truncated to the first, second, and third coefficient, respectively. The dashed curve corresponds to the semiempirical formulation of water vapor state. (See Ref. 21.)

association is responsible only for part of nonideal properties of water vapor because nonassociating molecules can also interact with each other and occupy a certain volume in space.

Accurate analytical analysis that takes into account non-ideal properties of monomolecular gas of each of the aforementioned water vapor constituents seems unfeasible at the present. However, their nonideal properties can be approximately taken into account employing, for instance, the Van der Waals equation of state that is accurate enough in the considered pressure range:

$$P(\rho) = \frac{\rho RT}{M - \rho b} - a \cdot \left(\frac{\rho}{M}\right)^2, \quad a = \frac{27(RT_c)^2}{64P_c}, \quad b = \frac{RT_c}{8P_c},$$

where  $\rho$  is gas density,  $M$  is molar mass,  $R$  is gas constant, and  $T_c$  and  $P_c$  are critical temperature and pressure, respectively. These critical parameters are, naturally, different for different constituents of water vapor. Nevertheless, because of similar physical origin of the constituents, it can be assumed that these critical parameters have close values for different constituents. So, the accurate values of  $T_c = 647.1$  K and  $P_c = 217.96$  atm corresponding to the monomer can also be used as approximate values for the dimer and trimer.

Using the equation of state one may obtain the reverse function  $\rho(P)$  and calculate the following density correction function:

$$Cr(P) = \frac{\rho(P)}{\rho^{id}(P)},$$

which is the ratio of densities of the ideal and real gas at the same pressure. We calculated the correction functions for all the three aforementioned water clusters and found that they are indistinguishable. More accurate correction function can be numerically calculated using the semiempirical formulation of water vapor state.<sup>21</sup> The function is shown in Fig. 2.

It should be noted that such density correction includes molecular association. We assume that the correction function taking into account nonideal properties of nonassociating constituents of water vapor should (i) lie somewhere in

between unity (the case of ideal gas) and the function shown in Fig. 2, and (ii) be a smooth function similar to the function in Fig. 2. So, the correction function for our modeling was constructed as

$$\text{Corr}(P) = (Cr(P) - 1) \cdot C + 1, \quad 0 < C < 1, \quad (4)$$

where  $C$  is the adjustable parameter of the model.

$$I = \frac{(P_m \text{Corr}(P_m) \cdot \sigma_m + P_d \text{Corr}(P_d) \cdot \sigma_d + P_t \text{Corr}(P_t) \cdot \sigma_t)}{kT}, \quad (5)$$

$$\alpha(\nu) = \frac{(P_m \text{Corr}(P_m) \sigma_m \Phi_m(\nu) + P_d \text{Corr}(P_d) \sigma_d \Phi_d(\nu) + P_t \text{Corr}(P_t) \sigma_t \Phi_t(\nu))}{kT}, \quad (6)$$

$$P \text{Corr}(P) = P_m \text{Corr}(P_m) + P_d \text{Corr}(P_d) + P_t \text{Corr}(P_t). \quad (7)$$

Here,  $k$  is Boltzmann constant,  $T$  is temperature, and  $P$  is the total pressure measured in the experiment. If we take into account that

$$P_d = K_d (P_m)^2, \quad P_t = K_t (P_m)^3 \quad (8)$$

( $K_d$  and  $K_t$  are dimer and trimer equilibrium constants), then the system of equations (7) and (8) allows finding partial pressures of monomer, dimer, and trimer through known values of  $P$ ,  $K_d$ , and  $K_t$ .

Density of the water vapor consisting of such a mixture can be written as

$$\rho = \frac{M}{RT} (P_m \text{Corr}(P_m) + 2P_d \text{Corr}(P_d) + 3P_t \text{Corr}(P_t)). \quad (9)$$

## B. Binary collisions approximation and impact approximation

These approximations in spectroscopy are assumed by default for molecular absorption modeling, in particular, for atmospheric absorption. Breakdown of the impact approximation in water vapor at elevated pressures was studied in experiments and compared to available models by

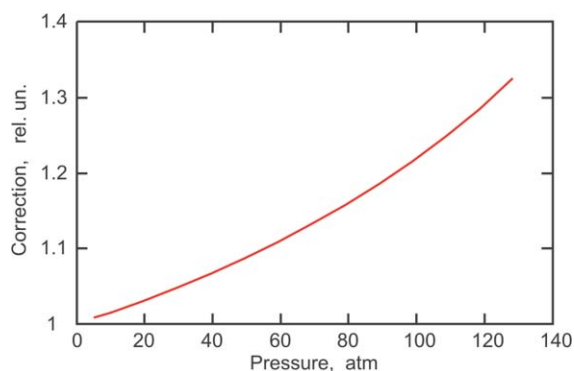


FIG. 2. Density correction function accounting for nonideal properties of water vapor at 650 K.

Bearing in mind that

$$n = \rho \frac{N_a}{M}, \quad \rho = \rho^{id} \text{Corr}(P) \text{ and } \rho^{id} = P \frac{M}{RT},$$

( $N_a = R/k$  is the Avogadro number) and neglecting water clusters higher than the trimer, one may transform Eqs. (1)–(3) to

Rieker *et al.*<sup>22</sup> It was shown that at 30 atms deviation from the Lorentz line shape reaches a few percent of the line amplitude. Validity of the binary collisions approximation can be checked by comparing the average time of molecule free flight between collisions with collision duration time. Free flight time can be estimated within the gas kinetic theory as the ratio of mean free path to average relative speed. Collision duration can be estimated as flight time through a distance equal to the diameter of a sphere of collisional interaction of molecules. The diameter can be roughly determined from an average line broadening parameter, which is rather well known for water lines.<sup>23</sup> At 650 K the collision duration and free flight times become equal at about 7.5 atms. The number of water molecules within the sphere of collisional interaction versus pressure is plotted in Fig. 3. This number is closely related to the estimation made above. It indicates that the experimental data are recorded under conditions which are beyond the limits of both approximations.

## C. Water dimer absorption band modeling

As was mentioned above, positions and intensities of all four O-H stretching bands of water dimer in the 3590–3800  $\text{cm}^{-1}$  range were experimentally determined in

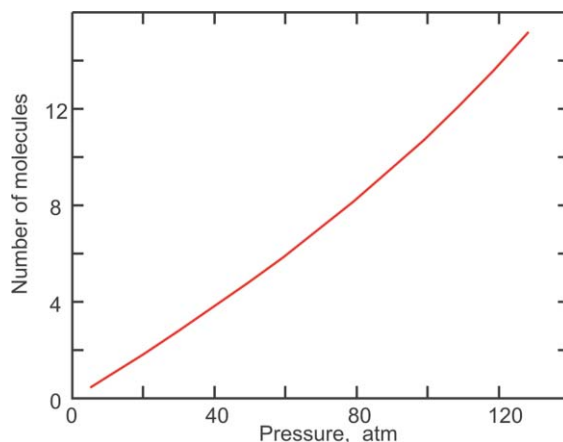


FIG. 3. Number of water molecules within spectroscopically determined sphere of collisional interaction vs pressure at 650 K.

He droplets.<sup>19</sup> No other dimer bands, including a possible combination band at  $3890\text{ cm}^{-1}$  discussed in Ref. 24, were observed up to  $3900\text{ cm}^{-1}$ .<sup>25</sup> According to the authors of Ref. 19, the measured position of the bands should correspond to the band positions in free dimers to an accuracy of  $\pm 4\text{ cm}^{-1}$  as a conservative estimate. Intensities of the bands were measured relative to the intensity of the  $\nu_3$  monomer band to an accuracy of 20%. Two more vibrational dimer modes corresponding to the first overtone of monomer bending fall into the frequency range of the experiment. Frequencies and intensities of these weak modes can be found from the theoretical paper by Kjaergaard *et al.*<sup>14</sup> These data are in a good agreement with the experimental observation of these dimer modes in neon matrix.<sup>24</sup> However, to avoid possible systematic only relative intensities of these modes from Ref. 14 were used in this work. Their absolute integrated intensities in the scale of intensities of Ref. 19 were found by comparing the corresponding data from the Refs. 14 and 19. Thus, the dimer absorption cross section ( $\sigma_d$ ) in the studied spectral range was determined.

The shape and width of the dimer band are uncertain. They are mainly determined by the inhomogeneous broadening resulting from overlapping of many separate lines. For modeling the dimer band we used the Lorentz profile of adjustable width. The same width was used for all dimer bands.

### D. Accounting for the water trimer absorption

Theoretical calculation of fundamental vibrations in the trimer can be found in Ref. 26, where positions and relative intensities of the fundamental O-H bound and O-H free vibrations are presented. The paper (Ref. 26) also contains a review of the corresponding experimental observations. The best agreement between the theoretical and the observed frequencies was achieved by optimizing parameters of calculated potential energy surface of the trimer. For our model, we used positions and relative intensities of these modes resulted from the optimization. Absolute intensity of the bands can be estimated using results of Slipchenko *et al.*,<sup>27</sup> where the O-H bound band of the trimer was observed in experiments in He droplets and its intensity was found. However, in the later work (Ref. 19) the authors slightly corrected the intensity of the dimer O-H bound band also measured in Ref. 27. So, to avoid systematic error we used the ratio of the intensities measured in those two works as a correction factor for the trimer O-H bound band intensity found in Ref. 27.

Similarly to the dimer, the Lorentz shape of adjustable width was used for each trimer band. Position and intensity of the dimer and trimer bands used in our model are listed in Table I.

### E. Modeling of the monomer spectrum taking into account line mixing (collisional coupling)

To the best of our knowledge there are no reported studies on manifestations of the mixing effect in the observed shapes of rovibrational bands of water vapor. Nevertheless, it is clear that the effect can be essential at pressures when all lines of rovibrational band blend together forming

TABLE I. Positions and integrated intensities of the dimer and trimer rovibrational bands used in the model.

Dimer <sup>a</sup>						
Position ( $\text{cm}^{-1}$ )	3193	3177	3597.4	3654.3	3730.1	3748.6
Intensity ( $\text{km/mol}$ )	5.9 <sup>b</sup>	0.75 <sup>b</sup>	144	4.5	96	44
Int. correction <sup>c</sup> (%)	0	0	+20	0	-20	-20
Trimer <sup>d</sup>						
Position ( $\text{cm}^{-1}$ )	3517	3532	3517	3693	3692	3693
Intensity ( $\text{km/mol}$ )	138	121.4	143.7	36.9	40.8	37.5
Int. correction <sup>c</sup> (%)	+20	+20	+20	+20	+20	+20

<sup>a</sup>Data are taken from Table II of Ref. 19.

<sup>b</sup>Data are taken from Table X of Ref. 14.

<sup>c</sup>Value of the intensity correction made at the final fitting step.

<sup>d</sup>Data are taken from Table III of Ref. 26. Intensities are recalculated using results of measurements from Ref. 27 and correction factor 1.07 as follows from Ref. 19.

structureless spectral feature. To account for the mixing effect in water monomer spectra it was decided to use a simple empirical adjustable branch coupling (ABC) approach developed by Tonkov *et al.*<sup>28</sup> The use of the approach assumes known positions, intensities, broadening parameters, and quantum numbers of all lines of the studied band. All this necessary information can be found, e.g., in the latest version of the high-resolution transmission molecular absorption (HITRAN) database.<sup>23</sup> The studied spectrum can be modeled with two adjustable parameters. The Lorentz profile was used for an individual line shape in spite of the limitations discussed in item “B.”

## III. DATA ANALYSIS

As stated in the Introduction, water vapor spectra recorded by Jin and Ikawa<sup>12</sup> were used for the analysis. The spectra in terms of absorbance ( $-\ln(E/E_0)$ , where  $E$  and  $E_0$  are the spectrometer signals recorded with and without gas, respectively) are presented in Fig. 4. They were recorded with  $2\text{ cm}^{-1}$  spectral resolution using a gas cell  $0.146\text{ cm}$  long. At the lowest experimental pressure (4.9 atm), the contribution of the dimer to the observed spectrum, as well as the contribution of the line mixing effect, is expected to be small. So this spectrum is good for testing the quality of modeling. The spectrum calculated with zero line mixing was convolved

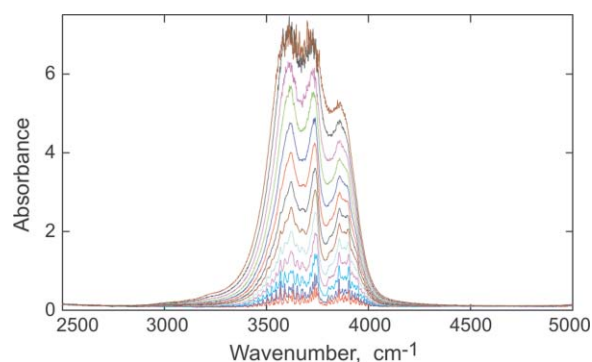


FIG. 4. Experimental spectra of water vapor absorption at 650 K and pressures from 4.9 up to 128 atm kindly supplied for the analysis by authors of Ref. 12.



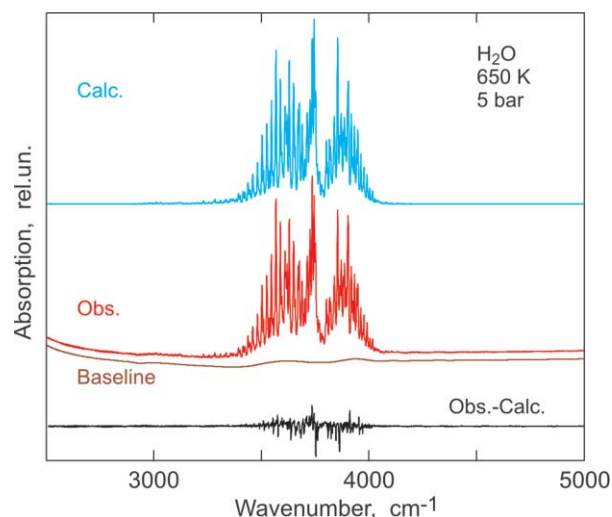


FIG. 5. Comparison of observed and calculated spectra at 4.9 atm.

with Gaussian function having  $2\text{-cm}^{-1}$  FWHM to account for instrumental resolution. The observed and calculated spectra are presented in Fig. 5.

The agreement is very good upon the whole. Detailed comparison revealed  $1\text{-cm}^{-1}$  systematic frequency shift of experimental spectrum and about 20% excess of the observed spectrum amplitude. The most probable reason of such amplitude divergence is inaccuracy of individual line parameters, including inaccuracy of their extrapolation to such extreme conditions. Another possible reason is a residual instrumental baseline problem. To proceed with the treatment the calculated spectrum amplitude was increased until minimum standard deviation of the difference between two spectra was achieved. This allowed accurate determination of the baseline, which was then subtracted from all experimental spectra. The baseline and the final difference between these two spectra are shown in Fig. 5. The difference gives some idea about accuracy of the modeling which, in our opinion, may be considered to be quite satisfactory.

Only the shape of the monomer spectrum ( $\Phi_m(\nu)$ ) calculated by the ABC model was used in further analysis to avoid systematic error related to the aforementioned underestimation of the calculated spectrum amplitude.

The integrated intensities of the observed spectra normalized by molecular concentration ( $I/n$ ) versus density are shown by points in Fig. 6. Clearly, at least two lowest and two highest points are affected by experimental peculiarities (the most probable reason, in our opinion, is the influence of noise at too low and too high optical depths) and should be omitted from the intensity analysis. The central part of the curve shows a very nice linear growth. Extrapolation of this dependence to zero concentration (the dashed line in Fig. 7) gives the water monomer absorption cross section  $\sigma_m = 55.6(3)$  km/mol. This value can be compared with the sum of intensities of all water lines in this spectral range at 650 K (note that allowance for natural abundance of water isotopes introduces negligible difference). This sum can be calculated using, for instance, various line lists contained in the database SPECTRA.<sup>29</sup> The recent HITRAN line list gives 50.1 km/mol and the Partridge–Schwenke line list gives 54.6 km/mol.

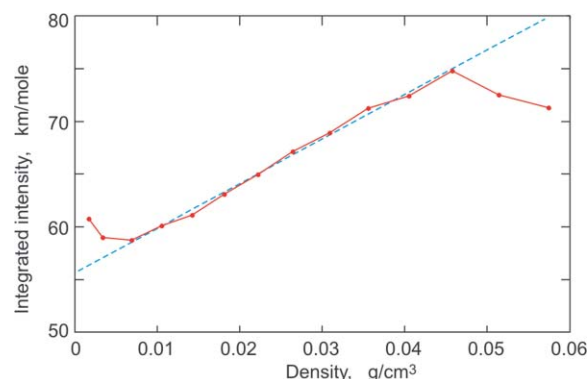


FIG. 6. Integrated intensity of observed water vapor spectra in the frequency range under consideration normalized by concentration (points) plotted vs density. The dashed line is linear regression of the data, excluding two upper and two lower points.

Similar calculation using the recent line list from Ref. 30 obtained on the base of the dipole moment surface from Ref. 31 yields 55.3 km/mol. So, the calculated data agree well with the experimental value mentioned above. Therefore, it can be used as a good starting point in further modeling of the spectra.

Thus, at this step we can, in principle, model using Eq. (6) a whole set of experimental data having only seven adjustable parameters, including dimer and trimer equilibrium constants, width of the dimer bands, width of the trimer bands, two parameters accounting for mixing of monomer lines and the parameter accounting for nonideal properties of nonassociating water vapor constituents. However, automatic minimization of the residual seems impractical because of the model roughness and strong correlation of its parameters. Therefore, in the first iteration we fitted the model manually (without the term accounting for the trimer) to several intermediate pressure (40–70 atm) spectra which should be less affected by the features of the experiment. This trial revealed that, with

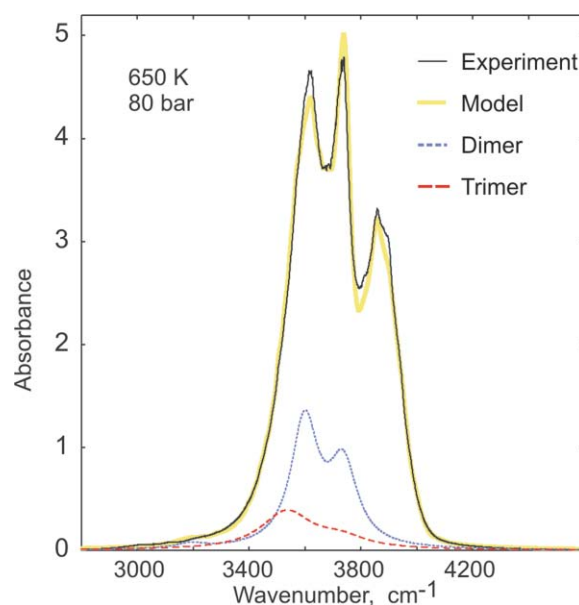


FIG. 7. Comparison of experimental and model spectra at 79 atm. Contributions of the dimer and trimer are shown by dashed curves.

reasonable values of adjustable parameters, the spectrum obtained by subtraction of the calculated monomer spectrum from the experimental one can be in a good coincidence with the expected spectrum of the dimer. The trial also revealed quite noticeable smooth residual absorption below  $3500\text{ cm}^{-1}$ . The absorption showed fast growth (even faster than  $P^3$ ) with the total pressure increase, indicating necessity of the trimer to be taken into account. So, at the next step the complete model [Eq. (6)] was used with initial values of adjustable parameters taken from the first step. Again, fully automatic fitting was not employed. Instead, we fitted spectra at intermediate pressures and checked whether the obtained constants are good for predicting spectra at other pressures. The integrated intensity model [Eq. (5)] and the correspondence of the density model [Eq. (8)] to the empirical data on the water vapor state<sup>21</sup> were used for an additional verification of the obtained equilibrium constants. It was found that the model is very sensitive to the value of the monomer absorption cross section. For example, with fixed values of adjustable parameters of the model 1% variation of the cross section value resulted in 8% change of the  $K_d$  value for similar description of the spectrum. Therefore, it was decided to allow for a small adjustment of  $\sigma_m$  at the final stage of fitting for better coincidence of observed and calculated spectra. At the final stage, we also varied within experimental uncertainty intensities of the major dimer and trimer bands, which also improved the quality of the fit. Relative values of the parameter corrections determined from the fitting are listed in Table I.

The observed and calculated water vapor spectra at 79 atm are compared in Fig. 7. Separate dimer and trimer contributions are also shown in Fig. 7. Figure 8 demonstrates the resulting evolution of the spectrum with an increase of pressure after subtraction of the calculated monomer contribution; model spectrum for the sum dimer and trimer contribution is also shown by the smooth line. The growth of the water vapor integrated intensity normalized by the concentration and monomer absorption cross section with increasing pressure is shown in Fig. 9 in comparison with experimental values. The contribution of each water vapor constituent is also shown in this figure.

The correspondence of the obtained data to the equation of state of water vapor is shown in Fig. 10. Final values of the model variable parameters are given in Table II.

#### IV. DISCUSSION

Figures 7–10 demonstrate that, in spite of all approximations and limitations, our model describes the observed spectra quite well. The dip in the absorption at  $3750\text{ cm}^{-1}$ , which is seen in Fig. 8, appeared as a result of imperfect allowance for the monomer contribution in the range of the sharp change of its absorption coefficient (see Fig. 7) where its modeling is most difficult.

Before making any conclusions on the results obtained let us consider definition of the dimer (and a similar definition of the trimer) assumed in this work. Strictly speaking, the dimer can be defined as a pair of interacting monomers. All the continuous spectrum of states from an orbiting collision of two

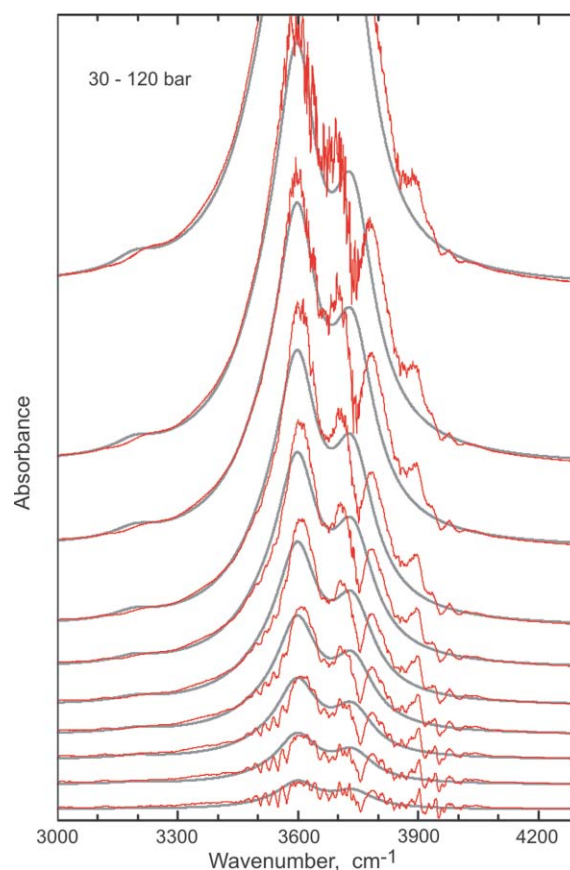


FIG. 8. Evolution of water vapor absorption spectrum after monomer subtraction. Pressure increment is 10 bar.

water molecules to a long lived water dimer satisfy this definition, especially at supercritical temperatures of water vapor.

In this paper, we consider the dimer as a highly flexible but still “normal” molecule in which two monomers are linked together by a hydrogen bond and the molecule

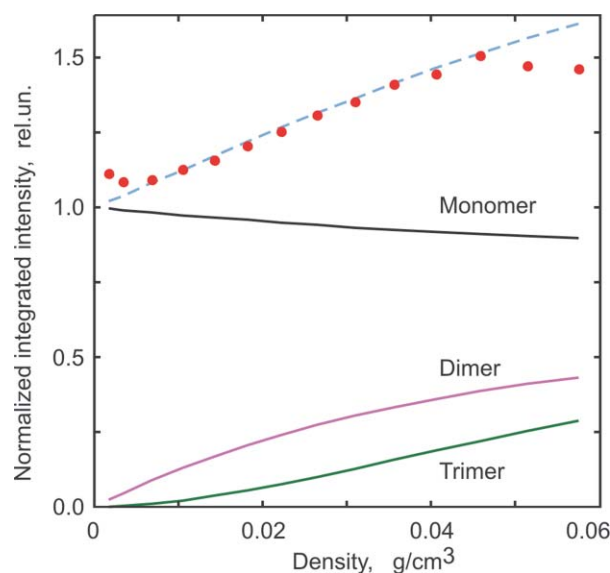


FIG. 9. Decomposition of integrated intensity of observed spectra. Growth of total integrated intensity of water vapor absorption calculated [Eq. (5)] with parameters from Table II vs pressure is shown by a dashed line. Experimental data are shown by points.

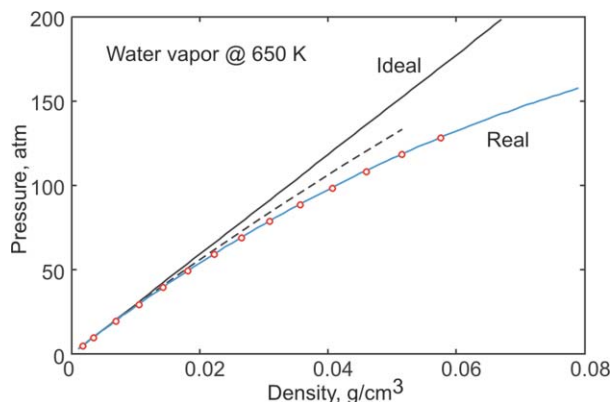


FIG. 10. Correspondence of the model to the equation of state of water vapor. Circles are calculated using Eq. (9) with parameters from Table II. Solid curves correspond to the equation of state for ideal and real vapor. Dashed line is calculated assuming that the vapor is a mixture of ideal monomer dimers and trimers [ $Corr(P) = 1$  in Eq. (9)].

rotates as a whole. The equilibrium structure of the dimer is known from observations in cold beams, and we assume that the structure does not change qualitatively in the conditions of the analyzed experiment. In fact, when fitting the model to the spectra we were looking for spectral manifestation of such bound molecules. In the conditions of the experiment there will be many highly excited quasibound or metastable states of the dimer (states with energies higher than the dimer dissociation energy  $D_0$ ), when the molecule still has almost the same structure and, therefore, almost the same absorption spectrum but additionally broadened by the state lifetime. Such states of the dimer are indistinguishable in our model from the true bound ones and, therefore, they contribute to the value of the dimer equilibrium constant found in this work. There will also be many others metastable states in which both monomers forming the dimer can rotate almost freely. The corresponding absorption spectrum should look more like the spectrum of a monomer broadened by a very short lifetime of such states. Such states are taken into account in our model by a correction for nonideal properties of monomers. The correction leads to a nonlinear increase of monomer concentration with increasing total pressure. Thus, such metastable states of the dimer contribute to the monomer absorption in our model.

The integrated intensities of the dimer bands measured at low temperatures were used in our model. Intermolecular vibrational modes in the dimer are thermally excited under the conditions of the considered experiment. The excitation increases the length of the hydrogen bond. This can lead to a decrease of the derivative of the dipole moment corresponding to O-H vibrations and, as a consequence, to a decrease

of the bands strength. The equilibrium dimer spectrum obtained in this work allows making some conclusions about possible decrease of the band intensities, which justifies usage of low temperature intensities. The dimer spectrum is shown in Fig. 7. The principal features of the spectrum are two peaks at about 3600 and 3700  $\text{cm}^{-1}$ . The peak at 3600  $\text{cm}^{-1}$  corresponds to the O-H bound local vibrational mode of the donor molecule. The peak at 3700  $\text{cm}^{-1}$  represents a sum of the O-H free local vibrational mode of the donor and antisymmetric stretch of the acceptor (assignment of peaks is taken in accordance with Ref. 14). The dimer vibrations strengths decreasing with thermal excitation still cannot become smaller than the strength of the corresponding vibrations in monomer. All the numbers for estimating the limits of the dimer peak intensity deviation can be found in Ref. 14, where results of calculation of the aforementioned vibrational modes by different models are presented in comparison with known experimental data. Such estimation shows that the peak at 3600  $\text{cm}^{-1}$  can decrease by about 2 orders of magnitude, whereas the peak at 3700  $\text{cm}^{-1}$  can become smaller only by 30–40%. Thus, very strong variation of peak amplitudes ratio with temperature is expected. The ratio of 3600–3700  $\text{cm}^{-1}$  peak amplitudes of a “cold dimer” calculated on the base of theoretical results<sup>14</sup> is within 1.21–2.11, depending on the model. In accordance with the experimental measurements,<sup>19</sup> the ratio for the cold dimer is within 0.69–1.54. The best fit of our model to the observed high temperature spectra was obtained with the ratio value of 1.54. This indicates that the aforementioned decrease of the vibration strength is not noticeable at least for a large fraction of dimers in water vapor in the conditions of the experiment.

It is interesting to compare the obtained value of the dimer equilibrium constant ( $0.87 \cdot 10^{-3} \text{ atm}^{-1}$  at 650 K) with the one known from the previous studies.

The upper limit of the constant can be determined from the second virial coefficient ( $B$ ):

$$K_d = -\frac{(B(T) - b)}{RT} = 2.1 \times 10^{-3} \text{ atm}^{-1},$$

where  $b$  is excluded volume (see the Van der Waals equation of state); for the constant calculation we used the value of  $B(T)$  obtained on the base of the experimental data [Eq. (6) and Table IV] of the paper by Harvey and Lemmon.<sup>32</sup> This value accounts for all  $P^2$ -related effects in water vapor and, therefore, all possible states of the dimer in its general definition as it was discussed above.

The  $K_d$  value, including its dependence on temperature in the 190–390 K range, was calculated in Ref. 13 by the quantum chemistry method. Only true bound states of the dimer (states with energies lower than  $D_0$ ) were taken into account. So, the value of the constant obtained in Ref. 13 can be treated in terms of our analysis as its lower limit. Extrapolation of these results to 650 K gives  $0.3 \times 10^{-3} \text{ atm}^{-1}$ .

The value of  $K_d$  was also calculated on the basis of the theory of associating systems by Evans and Vaida.<sup>33</sup> This calculation [Eq. (29)] from Ref. 33 and the result of recent calculation of  $D_0 = 1022 \text{ cm}^{-1}$  (Ref. 34) that has been corroborated in Ref. 15 at 650 K yields  $K_d = 0.5 \times 10^{-3} \text{ atm}^{-1}$ .

TABLE II. Values of equilibrium constants, widths of the dimer and trimer bands, monomer absorption cross section, and parameter of nonideal properties of nonassociating water vapor constituents as obtained from the fit of the spectra recorded at 650 K.

$K_d$ ( $\text{atm}^{-1}$ )	$K_t$ ( $\text{atm}^{-2}$ )	$\Delta\nu_d$ ( $\text{cm}^{-1}$ )	$\Delta\nu_t$ ( $\text{cm}^{-1}$ )	$\sigma_m$ ( $\text{km/mol}$ )	$C$ (rel.un.)
$0.87 \times 10^{-3}$	$2.2 \times 10^{-6}$	59	110	55.0	0.48



The most reliable experimental values of  $K_d$  were determined through measurements of water vapor thermal conductivity by Curtiss *et al.*<sup>35</sup> The principle of these measurements and quite high experimental temperatures (358–386 K) suggests noticeable integrated contribution of metastable states of the dimer to the found values of  $K_d$ , which is similar to our analysis. The values of  $K_d$  measured in Ref. 35 can be recalculated for other temperatures using the following equation:

$$K_d = \exp\left(\frac{\Delta S}{R} - \frac{\Delta H}{RT}\right),$$

where  $\Delta S$  and  $\Delta H$  are, respectively, the entropy and enthalpy of water dimer association, which were also determined in Ref. 35. For 650 K it yields  $K_d = 1.39 \times 10^{-3} \text{ atm}^{-1}$ .

Thus, the value of  $K_d$  obtained in our work is in a reasonable agreement with all the listed above values obtained from the previous studies. It is worth mentioning that exclusion of the trimer contribution from our model resulted in about 50%–70% increase of  $K_d$ , but decreased the quality of spectrum fitting significantly.

The width of the dimer rovibrational band was estimated to be  $59 \text{ cm}^{-1}$  (HWHM), which is almost two times larger than the widths of the spectral features potentially attributed to the dimer at near-room temperatures.<sup>7,36</sup> The trimer bands are found to be slightly less than twice broader than the dimer bands.

It is interesting that the  $3200\text{-cm}^{-1}$  dimer band at 650 K is shifted to higher frequencies by about  $20\text{--}30 \text{ cm}^{-1}$  in comparison to its low temperature position. The intensity of this weak band calculated in Ref. 14 exceeds the intensity measured in Ne matrix (Ref. 24) by about a factor of 2. It was found that the calculated intensity is in a better agreement with the observed high temperature spectra, so it was used in our model.

For description of high temperature spectra of water vapor at higher pressures the model should be improved, including (i) accounting for a breakdown of binary collisions and impact approximations; (ii) allowance for dimer and trimer bands narrowing due to line coupling evolving into rotational collapse, and (iii) accounting for higher-order water associates.

The manuscript of the paper was almost ready for submission when we found a very recent paper by Tassaing *et al.*<sup>37</sup> devoted to a similar subject. Experimental spectra of supercritical water were decomposed in Ref. 37 using a simple model at vapor densities much higher than those considered in our work. It is worth mentioning that, in spite of the different approaches, our results and the main findings of Ref. 37 are in a very good qualitative and even quantitative agreement. According to our model, water vapor at 650 K and 137 atm ( $0.063 \text{ g/cm}^3$ ) consists of 89% of monomer, 8.4% of dimer, and 2.6% of trimer. As can be determined from Fig. 7 of Ref. 37, the corresponding decomposition constitutes approximately 94%, 5%, and 1%, respectively. We also would like to point out a very good agreement between the integrated intensity of the experimental spectra used in our work and in Ref. 37. At 25 bar the intensity of the spectrum observed in

Ref. 37 in the fundamental O-H stretching region was found to be  $59 \pm 2 \text{ km/mol}$ . In our research, the corresponding intensity can be found using the dashed line in Fig. 7. It is  $59.3 \text{ km/mol}$ .

## V. CONCLUSIONS

The developed model [Eqs. (5)–(7)] describes rather well the spectra of high temperature water vapor in the O-H fundamental vibration range observed at densities up to about  $0.05 \text{ g/cm}^3$  on the base of the known high resolution spectrum of water monomer and positions and intensities of rovibrational bands of the dimer and the trimer measured in cold molecular beams. Extension of the model to higher density spectra requires accounting for higher-order water associates and spectroscopic modeling of rotational collapse.

The obtained value of the dimer equilibrium constant can serve as a reference for calculating the constant by modern methods of quantum chemistry. This value is in a good agreement with the previously known data. This indicates that the number of bound dimers in water vapor is quite large, even at such a high temperature, which implies that the observation of the dimer spectrum in equilibrium conditions at near-room temperature at millimeter waves proposed in Ref. 17 is feasible.

## ACKNOWLEDGMENTS

The authors express their deep gratitude to S. Ikawa for supplying experimental spectra for our analysis. We are also grateful to A. A. Vigasin and I. V. Ptashnik for valuable discussions and to N. N. Filippov for his fruitful critics of our preliminary results and his suggestion using the ABC model for line coupling accounting. Special gratitude is to A. F. Krupnov for initiating this study and for his permanent attention to it at all stages of the work. Partial support from the Russian Foundation for Basic Research, Institut de Physique, Centre National de la Recherche Scientifique (project PEPS-PTI), and from Swiss Secretariat for Education and Research (STCP-CH-RU research grant) is acknowledged.

<sup>1</sup>A. A. Viktorova and S. A. Zhevakin, Dokl Akad Nauk SSSR **171**, 1061 (1966).

<sup>2</sup>T. R. Duke and J. S. Muentner, J. Chem. Phys. **60**, 2929 (1974).

<sup>3</sup>F. N. Keutsch, N. Goldman, H. A. Harker, C. Leforestier, and R. J. Saykally, Mol. Phys. **101**, 3477 (2003); F. N. Keutsch, L. B. Braly, M. G. Brown, H. A. Harker, P. B. Petersen, C. Leforestier, and R. J. Saykally, J. Chem. Phys. **119**, 8927 (2003).

<sup>4</sup>H. A. Gebbie, W. J. Burroughs, J. Chamberlain, J. E. Harris, and R. G. Jones, Nature (London) **221**, 143 (1969).

<sup>5</sup>K. Pfeilsticker, A. Lotter, C. Peters, and H. Boesch, Science **300**, 2078 (2003).

<sup>6</sup>V. I. Serdyukov, L. N. Sinita, and Yu. A. Poplavskii, JETP Lett. **89**, 10 (2009).

<sup>7</sup>I. V. Ptashnik, J. Quant. Spectrosc. Radiat. Transf. **109**, 831 (2008); I. V. Ptashnik, K. P. Shine, and A. A. Vigasin, "Water vapour self-continuum and water dimers: 1. Analysis of recent work", J. Quant. Spectrosc. Radiat. Transf. (in press).

<sup>8</sup>V. Vaida, J. S. Daniel, H. G. Kjaergaard, L. M. Goss, and A. F. Tuck, Q. J. R. Meteorol. Soc. **127**, 1627 (2001).

<sup>9</sup>M. A. Stirkovich, G. V. Yuhnevitch, A. A. Vetrov, and A. A. Vigasin, Dokl Akad Nauk SSSR **210**, 321 (1973).

<sup>10</sup>G. V. Bondarenko and Yu. E. Gorbaty, Mol. Phys. **74**, 639 (1991).



- <sup>11</sup>T. Tassaing, Y. Danten, and M. Besnard, *Pure Appl. Chem.* **76**, 133 (2004).
- <sup>12</sup>A. A. Vigasin, Y. Jin, and S. Ikawa, *Mol. Phys.* **106**, 1155 (2008).
- <sup>13</sup>Y. Scribano, N. Goldman, R. J. Saykally, and C. Leforestier, *J. Phys. Chem. A* **110**, 5411 (2006).
- <sup>14</sup>H. G. Kjaergaard, A. L. Garden, G. M. Chaban, R. B. Gerber, D. A. Matthews, and J. F. Stanton, *J. Phys. Chem. A* **112**, 4324 (2008).
- <sup>15</sup>R. E. A. Kelly, J. Tennyson, and G. C. Groenenboom, *J. Quant. Spectrosc. Radiat. Transf.* **111**, 1262 (2010).
- <sup>16</sup>Y. Scribano and C. Leforestier, *J. Chem. Phys.* **126**, 234301 (2007).
- <sup>17</sup>A. F. Krupnov, M. Yu. Tretyakov, and C. Leforestier, *J. Quant. Spectrosc. Radiat. Transf.* **110**, 427 (2009).
- <sup>18</sup>M. Yu. Tretyakov, A. F. Krupnov, M. A. Koshelev, D. S. Makarov, E. A. Serov, and V. V. Parshin, *Rev. Sci. Instrum.* **80**, 093106 (2009).
- <sup>19</sup>K. Kuyanov-Prozument, M. Y. Choi, and A. F. Vilesov, *J. Chem. Phys.* **132**, 014304 (2010).
- <sup>20</sup>A. A. Vigasin, *Mol. Phys.* **108**, 2309 (2010).
- <sup>21</sup>W. Wagner and A. Pruss, *J. Phys. Chem. Ref. Data* **31**, 387 (2002); NIST Chemistry WebBook, available at: <http://webbook.nist.gov/chemistry/>.
- <sup>22</sup>G. B. Rieker, X. Liu, H. Li, J. B. Jeffries, and R. K. Hanson, *Appl. Phys. B* **87**, 169 (2007).
- <sup>23</sup>L. S. Rothman, I. E. Gordon, A. Barbe, D. C. Benner, P. F. Bernath, M. Birk, V. Boudon, L. R. Brown, A. Campargue, J.-P. Champion, K. Chance, L. H. Coudert, V. Dana, V. M. Devi, S. Fally, J.-M. Flaud, R. R. Gamache, A. Goldman, D. Jacquemart, I. Kleiner, N. Lacome, W. J. Lafferty, J.-Y. Mandin, S. T. Massie, S. N. Mikhailenko, C. E. Miller, N. Moazzen-Ahmadi, O. V. Naumenko, A. V. Nikitin, J. Orphal, V. I. Perevalov, A. Perrin, A. Predoi-Cross, C. P. Rinsland, M. Rotger, M. Simeckova, M. A. H. Smith, K. Sung, S. A. Tashkun, J. Tennyson, R. A. Toth, A. C. Vandaele, and J. Vander Auwera, *J. Quant. Spectrosc. Radiat. Transf.* **110**, 533 (2009). Available at: <http://www.cfa.harvard.edu/HITRAN>.
- <sup>24</sup>Y. Bouteiller and J. P. Perchard, *Chem. Phys.* **305**, 1 (2004).
- <sup>25</sup>A. F. Vilesov, private communication (22 January 2010).
- <sup>26</sup>T. Salmi, H. G. Kjaergaard, and L. Halonen, *J. Phys. Chem. A* **113**, 9124 (2009).
- <sup>27</sup>M. N. Slipchenko, K. E. Kuyanov, B. G. Sartakov, and A. F. Vilesov, *J. Chem. Phys.* **124**, 241101 (2006).
- <sup>28</sup>M. V. Tonkov, N. N. Filippov, Yu. M. Timofeev, and A. V. Polyakov, *J. Quant. Spectrosc. Radiat. Transf.* **56**, 783 (1996).
- <sup>29</sup>S. N. Mikhailenko, Yu. L. Babikov, and V. F. Golovko, *Atmos. Oceanic Opt.* **18**, 685 (2005). Available at <http://spectra.iao.ru/>.
- <sup>30</sup>S. V. Shirin, N. F. Zobov, R. I. Ovsyannikov, O. L. Polyansky, and J. Tennyson, *J. Chem. Phys.* **128**, 224306 (2008).
- <sup>31</sup>L. Lodi, R. N. Tolchenov, J. Tennyson, A. E. Lynas-Gray, S. V. Shirin, N. F. Zobov, O. L. Polyansky, A. G. Csaszar, J. van Stralen, and L. Visscher, *J. Chem. Phys.* **128**, 044304 (2008).
- <sup>32</sup>A. H. Harvey and E. W. Lemmon, *J. Phys. Chem. Ref. Data* **33**, 369 (2004).
- <sup>33</sup>G. T. Evans and V. Vaida, *J. Chem. Phys.* **113**, 6652 (2000).
- <sup>34</sup>C. Leforestier, R. van Harriet, and A. Van Der Avoird, *J. Chem. Phys. A* **113**, 12285 (2009).
- <sup>35</sup>L. A. Curtiss, D. J. Frurip, and M. Blander, *J. Chem. Phys.* **71**, 2703 (1979).
- <sup>36</sup>Yu. I. Baranov and W. J. Lafferty, "The water-vapor continuum and selective absorption in the 3 to 5  $\mu\text{m}$  spectral region at temperatures from 311 K to 363 K", *J. Quant. Spectrosc. Radiat. Transf.* (in press).
- <sup>37</sup>T. Tassaing, P. A. Garraïn, D. Bégué, and I. Baraille, *J. Chem. Phys.* **133**, 034103 (2010).